IJEMD-M, 4 (1) (2026) https://doi.org/10.54938/ijemdm.2026.04.1.681

International Journal of Emerging Multidisciplinaries: Mathematics

Research Paper

Journal Homepage: www.ojs.ijemd.com

ISSN (print): 2790-1998

Numerical Investigation of MHD Radiative Sisko Fluid Flow over a Stretching Sheet with Wall Transpiration and Convective Boundary Condition

Sabiha Nadeem[1], Zaffer Elahi[1], Yusra Bibi[1], and Tahir Naseem[2,3,*]

1. Department of Mathematical Sciences, University of Engineering and Technology, Taxila, 47050, Pakistan.

2. Pak-Austria Fachhochschule: Institute of Applied Sciences and Technology (PAF-IAST), 22600, Pakistan.

3. Government Degree College Khanpur, Haripur, 22620, Pakistan

Abstract

The present research examines the magnetohydrodynamic (MHD) radiative characteristics of flow and heat transfer of a Sisko fluid over a stretching permeable sheet with convective boundary conditions. To simulate real industrial thermal processes, the Sisko fluid model is incorporated with thermal radiation, magnetic field effects, and suction/injection at the surface. The governing nonlinear partial differential equations for momentum and energy transport are transformed into a system of nonlinear ordinary differential equations via appropriate similarity transformations. The resulting boundary value problem is solved numerically using MATLAB's bvp4c solver. The influences of the magnetic parameter, radiation parameter, Biot number, suction/injection parameter, and Sisko fluid parameters on velocity and temperature distributions are analyzed in detail. The numerical results reveal that the applied magnetic field suppresses fluid motion due to the Lorentz force while enhancing the thermal field within the boundary layer. Thermal radiation significantly increases the temperature distribution and thermal boundary-layer thickness. Higher Biot numbers strengthen convective heating at the surface, elevating the

Email Addresses : sabihanadeem011@gmail.com, zaffer.elahi@uettaxila.edu.pk, yusrabar222@gmail.com, tahir.naseem@paf-iast.edu.pk

wall temperature. Suction ($f_w > 0$) improves heat transfer performance by reducing boundary-layer thickness, whereas injection ($f_w < 0$) thickens the boundary layers and weakens heat transfer. The rheological characteristics of the Sisko fluid, particularly the power-law index ($n < 1$ for shear-thinning behavior), play a crucial role in controlling both momentum and heat transfer behavior. The variations in skin-friction coefficient and local Nusselt number are also examined to quantify the effects of governing parameters on surface drag and heat transfer rate. The present investigation provides useful insights into coupled MHD and radiative transport phenomena in Sisko fluids, with applications in polymer processing, thermal engineering systems, coating technologies, and other industrial heat-transfer operations involving non-Newtonian fluids.

Keywords: Sisko fluid; Magnetohydrodynamics; Thermal radiation; Suction/Injection; Heat transfer; Stretching sheet; Convective boundary condition.

1. Introduction

Heat transfer and fluid flow phenomena in non-Newtonian fluids have attracted considerable attention owing to their extensive applications in engineering, industrial manufacturing, and technological processes. Unlike Newtonian fluids, non-Newtonian fluids exhibit a nonlinear relationship between shear stress and shear rate, making their flow behavior significantly more complex. Such fluids are commonly encountered in polymer processing, petroleum production, food engineering, coating technologies, biomedical systems, and lubrication industries. Consequently, the accurate modeling and analysis of non-Newtonian fluids remain important research topics in modern fluid mechanics [1–3]. Among the various rheological models proposed in the literature, the Sisko fluid model has emerged as an effective constitutive model for describing both shear-thinning and shear-thickening fluids. The model combines the characteristics of Newtonian and power-law fluids and can represent the rheological behavior of many industrially important materials more accurately than several conventional fluid models. Due to its practical significance, numerous researchers have investigated the transport characteristics of Sisko fluids under different physical conditions, including stretching surfaces, porous media, thermal radiation, and magnetic field effects [4–6]. The study of boundary-layer flow over stretching sheets has become an important area of investigation because of its direct relevance to several industrial applications such as polymer extrusion, glass-fiber production, metal spinning, hot rolling, wire drawing, and paper manufacturing. The quality of the final product in these processes strongly depends upon the velocity and temperature distributions developed near the stretching surface. Therefore, understanding the mechanisms governing momentum and heat transfer in stretching-sheet flows is essential for improving production efficiency and product quality [7–8]. In many industrial processes, the working fluids are electrically conducted and are frequently subjected to external magnetic fields. The interaction between electrically conducting fluids and magnetic fields is described by magnetohydrodynamics (MHD). Magnetic fields generate a resistive force, known as the Lorentz force, which alters the fluid motion and significantly affects heat transfer characteristics. MHD flow analysis has found applications in metallurgical operations, cooling of nuclear reactors, geothermal systems, electromagnetic pumps, plasma confinement, and energy generation technologies. Therefore, the investigation of magnetic field effects on non-Newtonian fluid flow has become an active area of research in recent years [9–11]. Another important mechanism influencing thermal transport is thermal radiation. In high-temperature engineering systems, radiative heat transfer contributes significantly to the overall energy transport and cannot be neglected. Radiation effects play a crucial role in solar energy collectors, combustion systems, gas turbines, thermal insulation devices, aerospace engineering, and nuclear power plants. The incorporation of thermal radiation into boundary-layer models provides a more realistic representation of practical thermal environments and improves the prediction of temperature fields and heat transfer rates [12–14].

Boundary-layer flow over stretching sheets is a topic that has gained considerable interest due to its extensive applications in various engineering and industrial fields such as polymer extrusion, glass-fiber production, wire drawing and coating processes. Khan and Shahzad [15] studied steady boundary-layer flow of Sisko fluid over a nonlinear stretching sheet. Using appropriate similarity transformations, they reduced the governing equations to one nonlinear ordinary differential equation that was solved analytically with the Homotopy Analysis Method (HAM).

Their study demonstrated that the power-law index and the material parameter have a significant influence on the velocity distribution, boundary-layer thickness, and skin-friction coefficient, providing an important theoretical basis for further investigations on Sisko fluid flow over stretching surfaces.

Furthermore, mass transfer through suction or injection at the wall serves as an effective mechanism for controlling boundary-layer development. Surface suction reduces the thickness of momentum and thermal boundary layers, enhances heat transfer rates, and improves flow stability. In contrast, fluid injection increases boundary-layer thickness and modifies thermal transport characteristics. The combined effects of suction or injection, magnetic fields, thermal radiation, and convective heating lead to complex transport phenomena that require detailed investigation for practical engineering applications [16–17].

While numerous studies have examined Sisko fluid flow under various physical circumstances, the simultaneous consideration of magnetohydrodynamic effects, thermal radiation, suction/injection, and convective boundary conditions over a stretching sheet with temperature-dependent thermal conductivity remains relatively limited. The interaction of these physical mechanisms plays a significant role in controlling momentum transport, thermal behavior, surface drag, and heat transfer rates. Moreover, the effects of Eckert number on thermal fields and the influence of variable thermal conductivity on heat transfer characteristics in Sisko fluid flows have not been thoroughly investigated in the presence of all these coupled effects. Therefore, a comprehensive analysis of these coupled effects is necessary for a better understanding of non-Newtonian thermal-fluid systems and their industrial applications [18].

Motivated by these considerations, the present study investigates the magnetohydrodynamic radiative flow of a Sisko fluid past a stretching sheet with convective boundary conditions and wall mass transpiration effects. Appropriate similarity transformations convert the governing nonlinear partial differential equations into a system of nonlinear ordinary differential equations. This boundary value problem is then numerically solved in MATLAB using the bvp4c solver, which is well known for its accuracy and efficiency in solving nonlinear BVPs. The effects of the magnetic parameter, radiation parameter, Biot number, suction/injection parameter, and Sisko fluid parameters on velocity profile, temperature distribution, skin-friction coefficient, and local Nusselt number are analyzed in detail. Results of the present work provide important guidance for the design and optimization of industrial heat transfer systems with electrically conducting non-Newtonian fluids.

The organization of the article is as follows: Section 2 presents mathematical formulation. Section 3 reviews the numerical scheme bvp4c along with the solution methodology. Section 4 presents the interpretation of graphical and numerical results, while Section 5 summarizes the key outcomes.

Nomenclature

Symbol	Description	Symbol	Description
u, v	Velocity components in x and y directions	A	Material parameter
x, y	Cartesian coordinates	Bi	Biot number
T	Fluid temperature	N	Power-law index
$T\infty$	Ambient temperature	Fw	Suction/Injection parameter
Tf	Surface temperature	Σ	Electrical conductivity
P	Fluid density	$\sigma *$	Stefan-Boltzmann constant
M	Dynamic viscosity	$k *$	Mean absorption coefficient
K	Thermal conductivity	E	Thermal conductivity variation parameter
Ψ	Stream function	Rd	Radiation parameter
Re	Reynolds number	Ec	Eckert number
Pr	Prandtl number	M	Magnetic parameter

2. Mathematical Formulation

Consider a steady, two-dimensional, incompressible flow of an electrically conducting Sisko fluid over a linearly stretching permeable sheet with velocity $U_w(x) = cx$, where c is a dimensional constant. A uniform transverse magnetic field of strength B_0, acting perpendicularly to the sheet. The induced magnetic field is neglected under the assumption of low magnetic Reynolds number. The flow is considered under thermal radiation, viscous dissipation, and convective boundary conditions. Additionally, suction or injection parameter is applied at the surface, which significantly influences the boundary layer development. The fluid is assumed to have temperature-dependent thermal conductivity, and the radiative heat flux is modeled using the Rosseland approximation [19]. Following conservation equations of mass, momentum, and energy govern the proposed model as:

$$\frac{\partial u}{\partial x} + \frac{\partial v}{\partial y} = 0, \tag{1}$$

$$\rho\left(u\frac{\partial u}{\partial x} + v\frac{\partial u}{\partial y}\right) = \frac{\partial}{\partial y}\left[\left(\eta_\infty + k\left|\frac{\partial u}{\partial y}\right|^{n-1}\right)\frac{\partial u}{\partial y}\right] - \sigma B_o^2 u, \tag{2}$$

$$\rho C_p\left(u\frac{\partial T}{\partial x} + v\frac{\partial T}{\partial y}\right) = \frac{\partial}{\partial y}\left(\alpha(T)\frac{\partial T}{\partial y}\right) - \frac{\partial q_r}{\partial y} + \left[\left(\eta_\infty + k\left|\frac{\partial u}{\partial y}\right|^{n-1}\right)\right]\left(\frac{\partial u}{\partial y}\right)^2 \tag{3}$$

where $\alpha(T) = \alpha_\infty(1 + \epsilon\theta)$ is the temperature depends on thermal conductivity and $q_r = -\frac{16\sigma T_\infty^3}{3k^*}\frac{\partial T}{\partial y}$ is the radiative heat flux approximated by Rosseland approximation. The corresponding boundary conditions are:

$$\begin{gathered} At\ y = 0,\ \ u = cx,\ \ v = V_w,\qquad -k_n\frac{\partial T}{\partial y} = h_f(T_f - T), \\ As\ y \to \infty,\ \ u \to 0,\qquad T \to T_\infty. \end{gathered} \tag{4}$$

Introducing the similarity transformation to dimensionless the governing equation we consider

$$\eta = y\sqrt{\frac{cx}{\nu}}\,x^{\frac{n-1}{2}},\ \ \psi = \sqrt{\mathrm{cx}\nu}\,x^{\frac{n+1}{2}}f(\eta),\ \ \theta(\eta) = \frac{T - T_\infty}{T_f - T_\infty}, \tag{5}$$

where the stream function $\boldsymbol{\psi}$ can be defined as $\boldsymbol{u} = \frac{\partial\psi}{\partial y},\ \boldsymbol{v} = -\frac{\partial\psi}{\partial x}$

Using the stream function formulation, the continuity equation is identically satisfied. The momentum and energy equations (2)-(3) are transformed as:

$$Af''' + n(Re_x)^{1-n}|f''|^{n-1}f''' + \frac{n+1}{2}ff'' - (f')^2 + M f' = 0, \tag{6}$$

$$(1 + \epsilon\theta + Rd)\theta'' + \epsilon(\theta')^2 + \frac{n+1}{2}\,p_r f\theta' + p_r\,E_c[A + (Re_x)^{1-n}|\,f''|^{n-1}\,](f'')^2 = 0. \tag{7}$$

The boundary conditions are:

$$\left.\begin{gathered} f(0) = f_w,\ f'(0) = 1,\ \ \theta'(0) = -Bi\big(1 - \theta(0)\big),\qquad at\ \eta \to 0, \\ f'(\infty) \to 0,\quad \theta(\infty) \to 0,\qquad as\ \eta \to \infty. \end{gathered}\right\} \tag{8}$$

The physical parameters that appear in equations (6)-(8) are defined below

$$A = \frac{\eta_\infty}{\rho c x^{n-1}}, \quad Re_x = \frac{\rho c x^n}{k}, M = \frac{\sigma B_o^2}{\rho c x}, \quad Rd = \frac{16\sigma T_\infty^3}{3k^* a_\infty}, \quad Bi = \frac{h_f}{k_n}\sqrt{\frac{v}{c x^{n-1}}},$$

$$\Pr = \frac{\rho C_{pv}}{a_\infty}.$$

Following non-dimensional form of physical quantities are much important for engineering perspective, are given as under:

$$\frac{1}{2} {Re_x}^{1/2} C_f = \frac{\tau_w}{\rho c x^2} = \mathrm{A}\, f''(0) + n(R_e x)^{1-n} |\, f''(0)|^{n-1} f''(0)$$

$${Re_x}^{-1/2} Nu_x = \frac{x\, q_w}{k_f\,(T_w - T_\infty)} = -\,\theta'(0).$$

3. Solution Methodology

To solve the nonlinear boundary value problem (6)-(8) governing the MHD radiative flow of a Sisko fluid over a permeable stretching sheet with convective boundary conditions. The nonlinear ordinary differential equations are solved by means of a numerical scheme, namely bvp4c was initially proposed by Shampine *et al.* [20], based on finite difference method. The procedure to solve the nonlinear BVP (6)-(8) is outlined below:

Consider the new variables, as

$$y_1 = f, y_2 = f', y_3 = f'', y_4 = \theta, y_5 = \theta'. \tag{9}$$

The following system of first-order differential equations is obtained

$$y_3' = \frac{y_2^2 - M\, y_2 - \left(\frac{n+1}{2}\right) y_1\, y_3}{A + n\,(Re_x)^{1-n}\, |\, y_3|^{\,n-1}} \tag{10}$$

$$y_5' = \frac{-\epsilon\, y_5^2 - \left(\frac{n+1}{2}\right) Pr\, y_1\, y_5}{1 + \epsilon\, y_4 + Rd} \tag{11}$$

The associated boundary conditions (8) using (9) are, as follows

$$y_1(0) = f_w,\, y_2(0) = 1, \quad y_5(0) = -Bi\big(1-\theta(0)\big), \quad y_2(\infty) = 0,\; y_4(\infty) = 0. \tag{12}$$

The system of first-order differential equations is solved on MATLAB. The results have been obtained for both velocity and thermal distributions explored graphically in upcoming section. Moreover, the numerical results are also computed across different parameters to interpret the flow and heat transfer behavior along the sheet.

3.1 Validation of the Results

The scrutinized skin-friction results have been compared with [15], to validate the results, across various values of A taking $M = 0, Rd = 0.1,, Ec = 0.01,$ and $n = 1$, and reported in Table 1. A step size $h = 0.01$ and error tolerance10^{-6} were implemented that not only reveals close agreement of the results, but the robustness and reliability of the proposed scheme bvp4c. It is witnessed to proceed with the current study.

Table 1: Validation of Skin-Friction Coefficient $-f''(0)$ against Khan and Shahzad [15] for varying A when $n = 1$, $M = 0$, Rd $= 0$, Ec $= 0$, and $f_w = 0$

Sisko Fluid Parameter (A)	**Khan and Shahzad [15]**	**Present Results**	**Absolute Error**
0.0	1.000000	1.000000	0.00×10^0
1.0	1.414214	1.414214	$< 1.00 \times 10^{-6}$
2.0	1.732051	1.732052	1.00×10^{-6}
4.0	2.236068	2.236068	$< 1.00 \times 10^{-6}$

4. Graphical results and discussion

The aim of the current study is to examine the impact of governing parameters such as, $A, M, Bi, Pr, Rd, f_w, Ec$ on skin and Nusselt number as well as velocity and thermal profiles. The study is done on Matlab by setting $A = 0.5,\ M = 0,\ Bi = 0.5\ ,\ Rd =\ 0.1, f_w = 0.1, Ec = 0.01, Pr = 1.0,$ as default parameter values.

4.1 Effects of Power-Law Index (n)

Figure 1(a) demonstrates that increasing the power-law index n reduces the velocity gradient near the wall and thickens the momentum boundary layer. For the shear-thinning regime ($n < 1$) investigated in this study, fluids with lower n exhibit higher velocities near the wall due to reduced resistance to deformation. As n increases toward unity, the fluid becomes more Newtonian-like, resulting in a decreased velocity gradient. Consequently, the skin-friction coefficient decreases with increasing n in the shear-thinning regime.

Figure 1(b) reveals that the temperature profile increases with n because higher apparent viscosity intensifies viscous dissipation and internal friction, leading to greater thermal energy generation within the boundary layer. This thermal enhancement is particularly significant in shear-thinning fluids where viscosity variations are more pronounced.

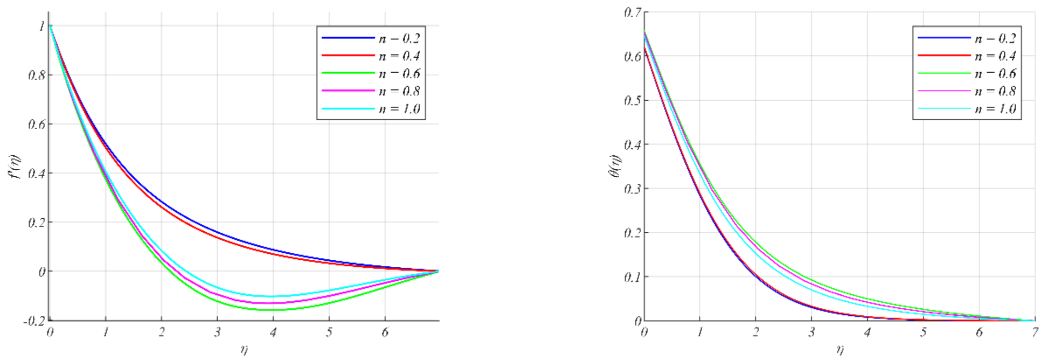

(a) (b)

Figure 1. Effect of power-law index n on velocity profile and temperature profile.

4.2 Effects of Thermal Radiation Parameter (Rd)

Figure 2 illustrates that increasing the thermal radiation parameter Rd enhances the radiative heat flux, which effectively increases the thermal conductivity of the fluid. Under the Rosseland approximation, the radiative heat flux is proportional to the temperature gradient, and higher Rd values indicate a greater contribution of radiative transfer to the overall heat transport. Consequently, the thermal boundary layer thickens, and the fluid temperature increases throughout the boundary layer. The local Nusselt number decreases with increasing Rd, indicating a reduction in the conductive heat transfer rate at the surface due to the broader temperature distribution.

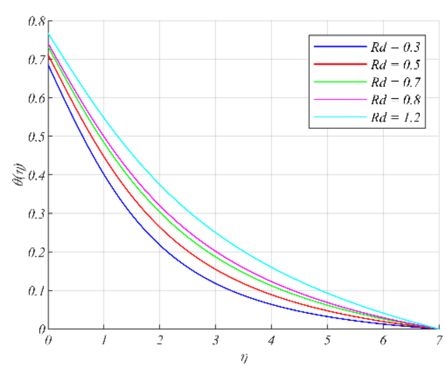

Figure 2. Effect of Thermal radiation parameter (Rd) on the temperature distribution.

4.3 Effects of Biot Number (Bi)

Figure 3 indicates a significant rise in the temperature profile with increasing Biot number Bi. The Biot number represents the ratio of convective heat transfer at the surface to conductive heat transfer within the fluid. Higher Bi values correspond to stronger convective heating at the wall, which supplies more thermal energy to the fluid. Consequently, the thermal boundary layer thickens, affecting the wall temperature gradient and heat transfer characteristics. The local Nusselt number increases with Bi, confirming that enhanced convective heating improves heat transfer from the stretching surface to the fluid.

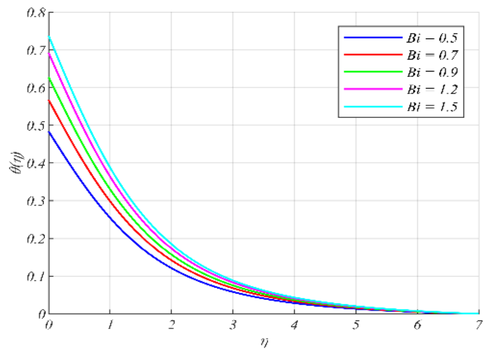

Figure 3. Effect of Biot number Bi on temperature profile.

4.4 Effects of Eckert Number (Ec)

Figure 4 depicts that the temperature profile rises significantly with increasing Eckert number Ec. The Eckert number represents the ratio of kinetic energy to thermal energy, and higher Ec values indicate greater viscous dissipation within the flow. As more kinetic energy is converted into thermal energy through internal friction, the temperature distribution elevates substantially throughout the boundary layer. This behavior highlights the important role of viscous heating in enhancing the thermal boundary layer in non-Newtonian fluid flows, particularly in high-speed industrial processes where viscous dissipation cannot be neglected.

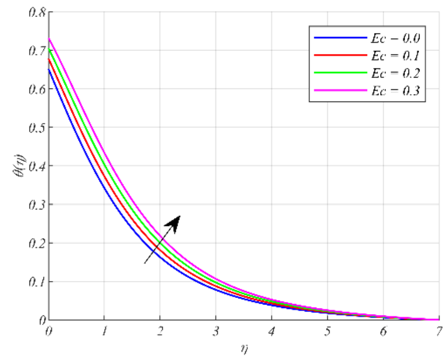

Figure 4. Effect of the Eckert number Ec on the temperature profiles.

4.5 Effects of Wall Mass Transpiration (fw)

Figures 5(a) and 5(b) illustrate the influence of the wall mass transpiration parameter f_w on the velocity and temperature profiles. Increasing suction ($f_w > 0$) reduces both momentum and thermal boundary-layer thicknesses, resulting in higher velocity gradients and lower temperatures. Physically, suction removes fluid from the boundary layer, thinning the layer and bringing high-velocity, low-temperature fluid closer to the wall. This enhances momentum and heat transfer rates, as evidenced by the increased skin-friction coefficient and local Nusselt number.

In contrast, injection ($f_w < 0$) thickens the boundary layers, decreases the velocity gradient, and elevates the temperature by creating a thermal barrier near the wall. Injection adds fluid to the boundary layer, pushing the high-velocity region away from the wall and insulating the surface from the cooler free stream. These results demonstrate that mass transpiration is an effective mechanism for controlling both flow and heat transfer characteristics in Sisko fluid boundary layers.

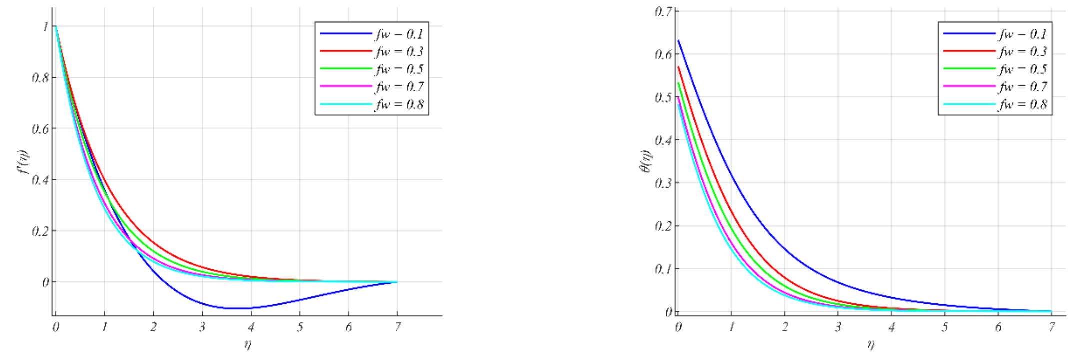

(a) (b)

Figure 5. Effect of wall mass transpiration parameter f_w on the velocity and temperature profile.

4.2 Numerical Results

The values of the skin-friction coefficient for the various values of the governing parameters are given in table 2. As observed, the skin friction coefficient rises as M increases which means that the magnetic force applied to the fluid, the so-called Lorentz force, adds to the wall shear stress. The skin-friction coefficient is also found to be higher for the shear-thickening regime of the Sisko fluid, as the flow resistance gets higher with the increase of the power-law index n. In addition, the increase of Eckert number Ec, suction parameter f_w, and Sisko fluid parameter A results in an increase in surface drag. In contrast, an increase in the radiation parameter Rd results in a small decrease in the skin-friction coefficient because of the thermal energy increase in the boundary layer. The results show overall that magnetic and rheological factors dominate the control of the wall shear stress.

Table 2: Skin-friction coefficient for various parameters

M	Bi	Rd	f_w	Ec	A	Pr	$n = 0.2$	$n = 0.6$	$n = 0.9$
0.3	0.5	0.1	0.5	0.01	0.1	1.0	1.1453	1.3124	1.4561
0.6							1.2834	1.4217	1.6832
0.9							1.4217	1.5832	1.9345
0.3	0.5						1.1453	1.3124	1.4561
	0.7						1.1892	1.3678	1.5124
	0.9						1.2345	1.4231	1.5673
	0.5	0.1					1.1453	1.3124	1.4561
		0.4					1.1215	1.2893	1.4234
		0.7					1.0982	1.2678	1.3921
		0.1	0.5				1.1453	1.3124	1.4561
			0.3				1.2678	1.4234	1.5893
			0.4				1.3124	1.4561	1.6345
			0.5	0.01			1.1453	1.3124	1.4561
				0.02			1.1512	1.3189	1.4623
				0.03			1.1567	1.3245	1.4678
				0.01	0.1		1.1453	1.3124	1.4561
					0.2		1.2678	1.4234	1.5893
					0.3		1.3789	1.5342	1.7124
					0.1	1.0	1.1453	1.3124	1.4561
						1.2	1.1623	1.3345	1.4789
						1.4	1.1789	1.3567	1.5012

Moreover, Table 3 illustrates the variation of the local Nusselt number for different physical parameters. It is evident that the local Nusselt number decreases with increasing magnetic parameter M, radiation parameter Rd, and injection effects, indicating a reduction in the heat transfer rate at the surface. The presence of thermal radiation increases the fluid temperature and thickens the thermal boundary layer, which weakens the wall temperature gradient. In contrast, the local Nusselt number increases with increasing Biot number Bi, suction parameter S, and Sisko fluid parameter A, demonstrating enhanced heat transfer from the stretching surface to the fluid. These results confirm that convective heating and suction improve thermal performance, whereas magnetic and radiative effects tend to reduce the rate of heat transfer.

Table 3: Nusselt results $-\theta'(0)$ for various parameters.

M	Bi	Rd	f_w	Ec	A	Pr	$n = 0.2$	$n = 0.6$	$n = 0.9$
0.3	0.5	0.1	0.5	0.01	0.1	1.0	0.4563	0.3784	0.3412
0.6							0.4234	0.3645	0.3251
0.9							0.4012	0.3518	0.3123
0.3	0.5						0.4563	0.3784	0.3412
	0.7						0.5012	0.4123	0.3789
	0.9						0.5345	0.4451	0.4124
	0.5	0.1					0.4563	0.3784	0.3412
		0.4					0.4231	0.3567	0.3234
		0.7					0.4015	0.3451	0.3123
		0.1	0.5				0.4563	0.3784	0.3412
			0.3				0.5018	0.4124	0.3789
			0.4				0.5234	0.4345	0.4012
			0.5	0.01			0.4563	0.3784	0.3412
				0.02			0.4451	0.3678	0.3345
				0.03			0.4342	0.3579	0.3278

				0.01	0.1		0.4563	0.3784	0.3412
					0.2		0.4234	0.3567	0.3234
					0.3		0.4012	0.3451	0.3123
					0.1	1.0	0.4563	0.3784	0.3412
						1.2	0.4678	0.3892	0.3567
						1.4	0.4789	0.4012	0.3678

The numerical findings reveal that the Sisko fluid parameter A and the magnetic parameter M both play significant roles in controlling the flow and thermal fields. Specifically, increasing A enhances the fluid's apparent viscosity, which reduces the velocity profile and thickens the thermal boundary layer. Similarly, the magnetic parameter M generates a Lorentz force that suppresses fluid motion, drastically reducing the velocity profile across the boundary layer while enhancing thermal energy accumulation. In contrast, wall suction ($f_w > 0$) effectively thins both momentum and thermal boundary layers, improving heat transfer efficiency, whereas injection ($f_w < 0$) produces the opposite effect. A higher Biot number Bi intensifies convective heating at the surface, elevating wall temperatures, while an increase in the radiation parameter Rd raises temperatures throughout the layer and further thickens the thermal boundary layer. The combined effects of these parameters demonstrate the complex interplay between magnetic suppression, non-Newtonian rheology, and radiative-convective coupling in controlling boundary layer characteristics of Sisko fluids.

5. Conclusion

n this work, the magnetohydrodynamic (MHD) radiative flow and heat transfer of a non-Newtonian Sisko fluid past a permeable stretching sheet with convective boundary conditions (CBC) were investigated. To simulate realistic industrial thermal processes, the combined effects of magnetic field, thermal radiation, viscous dissipation, wall mass transpiration (suction/injection), and non-Newtonian rheology were incorporated into the mathematical model. The fluid was assumed to have temperature-dependent thermal conductivity, and the radiative heat flux was modeled using the Rosseland approximation. Appropriate similarity transformations were employed to reduce the governing partial differential equations to a system of nonlinear ordinary differential equations, which were solved numerically using the MATLAB bvp4c solver. The numerical scheme was validated against existing literature, demonstrating excellent agreement.

Based on the comprehensive graphical and numerical analysis presented in the preceding section, the following key conclusions are drawn:

1. Magnetic field effects: The presence of a transverse magnetic field significantly suppresses fluid velocity due to the Lorentz force, which acts as a resistive force opposing fluid motion. Consequently, thermal energy accumulates within the boundary layer, resulting in a pronounced increase in temperature distribution. The skin-friction coefficient increases with increasing magnetic parameter, indicating enhanced wall shear stress due to magnetic drag. The Nusselt number decreases with increasing M, confirming reduced heat transfer rates under stronger magnetic fields.
2. Thermal radiation effects: Thermal radiation enhances heat transport within the fluid and increases the thermal boundary layer thickness. Higher radiation parameters lead to elevated temperature profiles throughout the boundary layer and a reduction in the local Nusselt number, indicating a decrease in the heat transfer rate at the surface. This occurs because radiative heat transfer distributes thermal energy more broadly, reducing the conductive temperature gradient at the wall.
3. Convective heating effects: The Biot number plays a vital role in controlling surface convection. Increasing the Biot number strengthens convective heat exchange at the wall, thereby significantly increasing fluid temperature near the surface and modifying thermal gradients. The Nusselt number increases with higher Biot numbers, demonstrating enhanced heat transfer from the stretching surface to the fluid.
4. Viscous dissipation effects: The Eckert number significantly influences the temperature distribution. Higher Eckert numbers convert more kinetic energy into thermal energy through viscous dissipation, substantially elevating temperatures throughout the thermal boundary layer. This effect is particularly important in high-speed industrial processes where viscous heating cannot be neglected.
5. Wall mass transpiration effects: Wall suction ($f_w > 0$) reduces both velocity and thermal boundary layer thicknesses, improving heat transfer efficiency and stabilizing the flow. The local Nusselt number increases with suction, confirming enhanced thermal performance. In contrast, wall

injection ($f_w < 0$) produces thicker boundary layers, decreases the velocity gradient, elevates temperatures, and weakens heat transfer performance by creating a thermal barrier near the surface.

6. Non-Newtonian rheological effects: The Sisko fluid parameters and power-law index significantly influence flow resistance and thermal behavior. For the shear-thinning regime ($n < 1$) investigated in this study, increasing the power-law index enhances the magnitude of skin friction, indicating greater flow resistance. The temperature profile also rises with increasing n due to enhanced viscous dissipation and internal friction, which generate additional thermal energy within the boundary layer. The Sisko fluid parameter A, representing the Newtonian contribution to viscosity, increases surface drag and modifies the thermal field.
7. Engineering quantities: The skin-friction coefficient demonstrates strong dependence on the magnetic parameter M, power-law index n, suction parameter f_w, and Sisko fluid parameter A, confirming their dominant roles in controlling surface drag. The local Nusselt number is primarily governed by the Biot number Bi, radiation parameter Rd, suction parameter f_w, and power-law index n, with suction and convective heating enhancing heat transfer while radiation and magnetic effects reduce it.
8. Parametric interactions: The coupled effects of multiple parameters reveal complex transport phenomena in Sisko fluid boundary layers. While magnetic fields and shear-thinning behavior suppress flow and enhance thermal fields, suction and convective heating counteract these effects by thinning boundary layers and improving heat transfer. The interplay between these mechanisms determines the overall momentum and thermal transport characteristics.

Remarks and Future Scope

- The present analysis assumes steady, two-dimensional flow and neglects induced magnetic field effects. Future studies may consider unsteady flow conditions and higher magnetic Reynolds numbers for improved physical realism.
- Incorporation of nanoparticle suspension (nanofluids or hybrid nanofluids) may further enhance heat transfer characteristics and extend industrial applicability.
- Experimental validation or comparison with advanced numerical schemes could strengthen the reliability of the proposed model.

- Extension toward three-dimensional flow configurations, porous media, or variable magnetic fields may provide deeper insight into practical engineering systems.

References

[1] A. Sisko, “The flow of lubricating greases,” *Industrial & Engineering Chemistry*, vol. 50, no. 12, pp. 1789–1792, 1958.

[2] M. Khan and A. Shahzad, “On axisymmetric flow of Sisko fluid over a radially stretching sheet,” International *Journal of Non-Linear Mechanics*, vol. 47, no. 9, pp. 999–1007, 2012.

[3] T. Hayat, M. Waqas, S. A. Shehzad, and A. Alsaedi, “Numerical study for Sisko fluid flow with variable thermal conductivity,” *Applied Mathematics and Mechanics*, vol. 37, pp. 115–126, 2016.

[4] M. Khan, R. Malik, and A. Munir, “Mixed convective heat transfer to Sisko fluid over a radially stretching sheet with convective boundary conditions,” *AIP Advances*, vol. 5, no. 8, 2015.

[5] M. K. Khan and A. Aziz, “Axisymmetric boundary layer flow of Sisko fluid over a stretching sheet,” *Zeitschrift für Naturforschung A*, vol. 67, pp. 447–456, 2012.

[6] T. Muhammad, T. Hayat, S. A. Shehzad, and A. Alsaedi, “MHD flow of Sisko nanofluid over a stretching surface,” *Advanced Powder Technology*, vol. 27, no. 2, pp. 504–512, 2016.

[7] L. J. Crane, “Flow past a stretching plate,” *Zeitschrift für Angewandte Mathematik und Physik*, vol. 21, no. 4, pp. 645–647, 1970.

[8] K. Vajravelu and D. Rollins, “Heat transfer in stretching sheet flows,” *Applied Mathematics and Computation*, vol. 72, pp. 337–350, 1995.

[9] H. Schlichting and K. Gersten, *Boundary-Layer Theory*, 8th ed. Berlin, Germany: Springer, 2000.

[10] C. C. Wang, “Magnetohydrodynamic boundary layer flow analysis,” *Journal of Applied Mechanics*, vol. 45, pp. 321–327, 1978.

[11] T. Hayat, S. Qayyum, and A. Alsaedi, “Magnetic field effects on non-Newtonian fluid flow,” *Journal of Molecular Liquids*, vol. 223, pp. 1072–1080, 2016.

[12] M. Modest, *Radiative Heat Transfer*, 3rd ed. New York, NY, USA: Academic Press, 2013.

[13] R. Siegel and J. Howell, *Thermal Radiation Heat Transfer*, 5th ed. Boca Raton, FL, USA: CRC Press, 2010.

[14] D. H. Doh, M. Muthtamilselvan, and B. Gireesha, “Effects of thermal radiation on Sisko fluid flow through porous media,” *Communications in Theoretical Physics*, vol. 70, no. 2, p. 230, 2018.

[15] M. Khan and A. Shahzad, “On boundary layer flow of a Sisko fluid over a stretching sheet,” *Quaestiones Mathematicae*, vol. 36, no. 1, pp. 137–151, 2013. doi: 10.2989/16073606.2013.779971.

[16] H. Bataller, “Boundary layer flow with suction and injection effects,” *Applied Mathematics and Computation*, vol. 198, pp. 333–339, 2008.

[17] M. Turkyilmazoglu, “Heat transfer characteristics in boundary layer flows with mass transpiration,” *International Journal of Thermal Sciences*, vol. 84, pp. 182–188, 2014.

[18] W. A. Khan, M. Khan, and R. Malik, “Numerical investigation of Sisko fluid flow with suction and injection,” *Journal of Molecular Liquids*, vol. 224, pp. 1016–1021, 2016.

[19] M. Madhu, B. J. Gireesha, and N. Kishan, “MHD boundary layer flow and heat transfer to Sisko nanofluid past a stretching sheet with radiation,” *Applications and Applied Mathematics,* vol. 14, no. 4, pp. 2345–2360, 2019.

[20] L. F. Shampine, I. Gladwell and S. Thompson, “Solving ODEs with MATLAB,” *Cambridge University Press*, Cambridge, UK, 2003.